PERIODICA POLYTECHNICA SER. EL. ENG. VOL. 46, NO. 1–2, PP. 15–28 (2002)

INVESTIGATION OF INDUCTION HEATING OF NON-FERROMAGNETIC METAL HALF-SPACE WITH CORRUGATED SURFACE: THE EXCITING MAGNETIC FIELD IS PERPENDICULAR TO THE PLANE OF THE CORRUGATED PROFILE.

László KOLLER, György TEVAN and István KISS

Department of High Voltage Engineering and Equipment
Budapest University of Technology and Economics
H–1521 Budapest Hungary
e-mails: koller@ntb.bme.hu, tevan@ntb.bme.hu, kiss@ntb.bme.hu

Received: April 25, 2002

Abstract

In this paper the electromagnetic field of a metal half-space with corrugated surface is investigated in the case where the exciter magnetic field is perpendicular to the plane of the corrugated profile. The partial differential equation of the two-dimensional field computation was solved using linear base functions, exactly fulfilling the differential equations, while the coefficients were determined to fulfil the boundary conditions approximately. A computer program was made to analyse the effect of different parameters.

Keywords: induction heating, corrugated metal surface.

1. Introduction

The efficiency of induction heating is higher if the resistance of the heated load with invariance of the resistance of the inductor coil is higher. *Enlarging the length of the eddy current course* raises the resistance of the charge and, thus, the efficiency. Therefore it is suitable to investigate the quantity relations in metal load with *corrugated surface*. The simplest model is a *half-space* metal with a *sinusoidal* wave-form surface, and increase of the length of the eddy current course can be developed if the exciting magnetic field is perpendicular to the plane of the corrugated profile.

2. The Mathematical Model

Fig. 1 shows the arrangement of the model in a Descartes co-ordinate system. The domain with notation ‘air gap’ can be another non-metal material as well. From the model and from the arrangement of the excitation follows that field quantities are

independent of the co-ordinate z, the magnetic field strength has only z-component, and the electric field strength has no z-component:

$$\frac{\partial}{\partial z} = 0, \quad \mathbf{H} = \mathbf{H}_z, \quad \mathbf{E}_z = \mathbf{0}. \tag{1}$$

Here and in the following the bold type letters note (complex) phasors according to the sinusoidal time-dependent excitation with frequency ω. Because at usual frequencies and with usual air-gap depth the displacement current can be neglected, therefore the Maxwell equations in the load are:

$$\frac{\partial \mathbf{H}}{\partial x} = -\sigma \mathbf{E}_y, \tag{2}$$

$$\frac{\partial \mathbf{H}}{\partial y} = \sigma \mathbf{E}_x, \tag{3}$$

where σ is the conductivity of the load. In the air gap the field equations have the form:

$$\frac{\partial \mathbf{H}}{\partial x} = \mathbf{0} \quad \text{and} \quad \frac{\partial \mathbf{H}}{\partial y} = \mathbf{0}. \tag{4}$$

According to (1) also $\dfrac{\partial \mathbf{H}}{\partial z} = \mathbf{0}$ is valid, therefore in the air gap

$$\mathbf{H} = \text{const.} = H_0, \tag{5}$$

and this is the magnetic field intensity excited by inductor current I.

In the load the second Maxwell equation takes the following form:

$$\frac{\partial \mathbf{E}_y}{\partial x} - \frac{\partial \mathbf{E}_x}{\partial y} = -j\omega\mu_0 \mathbf{H}. \tag{6}$$

Substituting (2) and (3) into (6) we obtain the following partial differential equation:

$$\frac{\partial^2 \mathbf{H}}{\partial x^2} + \frac{\partial^2 \mathbf{H}}{\partial y^2} = j\omega\mu_0\sigma \mathbf{H} \equiv \frac{2j}{\delta^2}\mathbf{H}, \tag{7}$$

where

$$\delta = \sqrt{\frac{2}{\sigma\omega\mu_0}} \tag{8}$$

is the skin depth.

The boundary conditions are:

a., On the basis of (5), along the boundary surface between the air gap and metal,

$$\text{at } x = x_p(y) \equiv a + \frac{h}{2}\left[1 + \cos\left(\frac{2\pi y}{l}\right)\right], \quad \mathbf{H} = H_0. \tag{9}$$

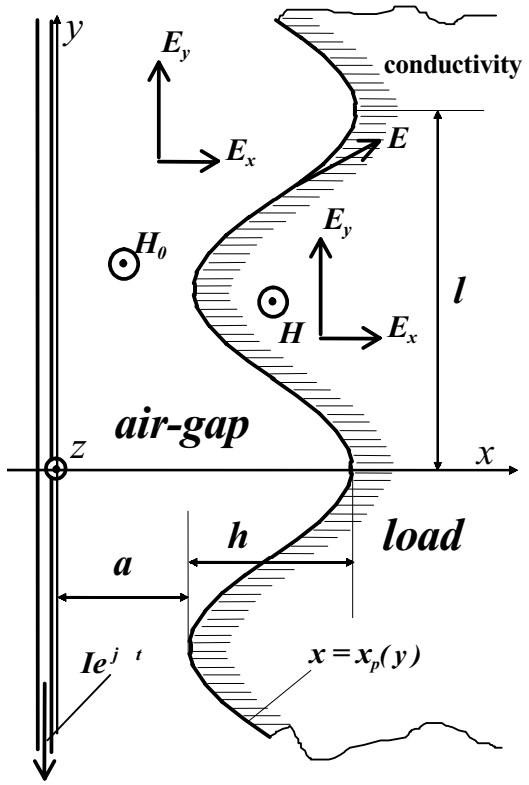

Fig. 1.

This condition also guarantees that currents do not enter from the metal load into the air gap along the rippled surface. Namely, according to the Amper law written for this surface, the relation $\oint H_0\vec{e}_z \,\mathrm{d}\vec{s} = H_0\vec{e}_z \oint \mathrm{d}\vec{s} = 0$ is valid. ($\vec{e}_z$ is unit vector, directed in z-axis.)

b., Because of the half-space, the magnetic field intensity has to fulfil the regularity condition

$$\text{at } x \to \infty \quad \mathbf{H} \to \mathbf{0}. \tag{10}$$

c., As a consequence of the periodicity in direction y it is sufficient to calculate the field in the interval $0 \le y \le l$, but the following symmetry condition must be satisfied:

$$\mathbf{H}\,(x, l-y) = \mathbf{H}\,(x, y)\,. \tag{11}$$

On the basis of (3), relation $\mathbf{E}_x(x, l-y) = -\mathbf{E}_x(x, y)$ is valid, and so relation $\mathbf{E}_x(x, l) = -\mathbf{E}_x(x, 0)$ is valid as well.

d., As a consequence of the periodicity, *all of the field quantities* must be taken with the same value into consideration, therefore the last relation leads to the

condition

$$\mathbf{E}_x(x,0) = \mathbf{0}. \tag{12}$$

3. The Solution

The solution is investigated only in the metal load, because the magnetic field strength in the air gap according to (5) is known, H_0. It seems suitable to seek the solution in the metal in form of Fourier series, where, on the basis of (11), it is prescribed only by cosine terms:

$$\mathbf{H} = \sum_{\mathbf{n}=0}^{N-1} \mathbf{w}_n(x) \cos\left(n\frac{2\pi}{l}y\right). \tag{13}$$

With this condition (12) is satisfied as well, as it can be seen from formula (3). Substituting expression (13) into the differential equation (7) we get for the functions $\mathbf{w}_n(x)$:

$$\mathbf{w}''_{\mathbf{n}}(x) = \left[\frac{2j}{\delta^2} + \left(\frac{2\pi}{l}n\right)^2\right]\mathbf{w}_{\mathbf{n}}(x). \tag{14}$$

Introducing the notation

$$\mathbf{q}_n = \sqrt{2j + \left(2\pi n\frac{\delta}{l}\right)^2}, \quad \mathrm{Re}(\mathbf{q}_n) > 0, \tag{15}$$

the solution of differential equation (14) is under condition (10):

$$\mathbf{w}_n(x) = \mathbf{C}_n e^{-\mathbf{q}_n\frac{x-a}{\delta}}, \quad (n = 0, 1, 2, 3, \ldots N-1).$$

So (13) has the following form:

$$\mathbf{H} = \sum_{n=0}^{N-1} \mathbf{C}_n e^{-\mathbf{q}_n\frac{x-a}{\delta}} \cos\left(n\frac{2\pi}{l}y\right). \tag{16}$$

Coefficients $\mathbf{C}_n$ are selected so that they satisfy condition (9).

However, at $x = \text{constant} < a + h$ the metal load is not continuous (see *Fig. 1*), so the y-functions in (16) do not compose a complete set of function series. Therefore a complement series satisfying differential equation (7) and boundary condition (10) is introduced and making complete set in variable x. If the factor depending on x in the terms of the complement series has the form $e^{\boldsymbol{t}_n\frac{x-a}{\delta}}$, with

$$\boldsymbol{t}_n = -\tau_1 + n\tau_2 j, \quad \text{where} \quad \tau_1 > 0, \quad \tau_2 > 0, \tag{17}$$

then condition (10) is satisfied. Substituting $e^{\mathbf{t}_n \frac{x-a}{\delta}}\mathbf{v}_n(y)$ into (7) the following ordinary differential equation is obtained:

$$\mathbf{v}_n''(y) = \left(\frac{2j}{\delta^2} - \frac{\mathbf{t}_n^2}{\delta^2}\right)\mathbf{v}_n(y) \equiv \frac{\mathbf{p}_n^2}{\delta^2}\mathbf{v}_n(y),$$

where

$$\mathbf{p}_n = \sqrt{2j - \mathbf{t}_n^2} = \sqrt{n^2\tau_2^2 - \tau_1^2 + 2j\,(1 + n\tau_1\tau_2)}, \quad \mathrm{Re}\,(\mathbf{p}_n) > 0. \tag{18}$$

So the complement series is an x-directional damping Fourier series. Afterwards it can be seen that it will lead to a good result since the algorithm and the program calculate the relative average error of the fulfilling of boundary conditions and that value is appropriately small in the given cases. (See later results.)

The solution of previous differential equation accomplishing also symmetry condition (11) has the form:

$$\mathbf{v}_n\,(y) = e^{\frac{\mathbf{p}_n}{\delta}\left(y-\frac{l}{2}\right)} + e^{-\frac{\mathbf{p}_n}{\delta}\left(y-\frac{l}{2}\right)}.$$

Thus, the formula for the magnetic field intensity (16) has to be completed in the following way:

$$\mathbf{H} = \sum_{n=0}^{N-1} \mathbf{C}_n e^{-\mathbf{q}_n \frac{x-a}{\delta}} \cos\left(n\frac{2\pi}{l}y\right)$$
$$+ \sum_{n=N}^{N+M-1} \mathbf{C}_n \left[e^{\frac{\mathbf{p}_n}{\delta}\left(y-\frac{l}{2}\right)} + e^{-\frac{\mathbf{p}_n}{\delta}\left(y-\frac{l}{2}\right)}\right] e^{\mathbf{t}_n \frac{x-a}{\delta}} \equiv \sum_{n=0}^{N+M-1} \mathbf{C}_n \mathbf{H}_n. \tag{19}$$

The expressions for the electric field strength components can be got by substituting

(19) into (2) and (3):

$$\begin{aligned}\mathbf{E}_x &= -\frac{2\pi}{l\sigma}\sum_{n=1}^{N-1} n\mathbf{C}_n e^{-\mathbf{q}_n\frac{x-a}{\delta}}\sin\left(n\frac{2\pi}{l}y\right)\\ &\quad+\frac{1}{\delta\sigma}\sum_{n=N}^{N+M-1}\mathbf{C}_n\mathbf{p}_n\left[e^{\frac{\mathbf{p}_n}{\delta}(y-\frac{l}{2})}-e^{-\frac{\mathbf{p}_n}{\delta}(y-\frac{l}{2})}\right]e^{\mathbf{t}_n\frac{x-a}{\delta}}\\ &\equiv\sum_{n=0}^{N+M-1}\mathbf{C}_n\mathbf{E}_{xn},\\ \mathbf{E}_y &= \frac{1}{\delta\sigma}\sum_{n=0}^{N-1}\mathbf{q}_n\mathbf{C}_n e^{-\mathbf{q}_n\frac{x-a}{\delta}}\cos\left(n\frac{2\pi}{l}y\right)\\ &\quad-\frac{1}{\delta\sigma}\sum_{n=N}^{N+M-1}\mathbf{C}_n\mathbf{t}_n\left[e^{\frac{\mathbf{p}_n}{\delta}(y-\frac{l}{2})}+e^{-\frac{\mathbf{p}_n}{\delta}(y-\frac{l}{2})}\right]e^{\mathbf{t}_n\frac{x-a}{\delta}}\\ &\equiv\sum_{n=0}^{N+M-1}\mathbf{C}_n\mathbf{E}_{yn}.\end{aligned}\tag{20}$$

Complex coefficients $\mathbf{C}_n$ must be selected so that the error in satisfying boundary conditions (9) and (12) be as small as possible. For this an integral of the square of the error along the wave surface at condition (9) and along the surface $y = 0$ at the condition (12) is developed and minimised. Thus, the minimum of the expression

$$W=\int_{y=0}^{\frac{l}{2}}\left|\sum_{n=0}^{N+M-1}\mathbf{C}_n\left(\mathbf{H}_n\right)_{x=x_p(y)}-H_0\right|^2\mathrm{d}y+\lambda\int_{x=a+h}^{\infty}\left|\sum_{n=N}^{N+M-1}\mathbf{C}_n\left(\mathbf{E}_{xn}\right)_{y=0}\right|^2\mathrm{d}x\tag{21}$$

results the required coefficients $\mathbf{C}_n$. Here λ is a suitable positive constant. (In the first term of the expression the symmetry, in the second term the fact has been utilised that for $n < N$ $\mathbf{E}_{xn} = 0$.) Searching the minimum of formula W in (21) leads to the solution of the complex linear system of equations for $\mathbf{C}_n$:

$$\begin{aligned}&\int_{y=0}^{\frac{l}{2}}\left[\sum_{n=0}^{N+M-1}\mathbf{C}_n\left(\mathbf{H}_n\right)_{x=x_p(y)}-H_0\right]\left[\left(\mathbf{H}_k\right)_{x=x_p(y)}\right]^*\mathrm{d}y\\ &+\lambda\int_{x=a+h}^{\infty}\left[\sum_{n=N}^{N+M-1}\mathbf{C}_n\left(\mathbf{E}_{xn}\right)_{y=0}\right]\left[\left(\mathbf{E}_{xk}\right)_{y=0}\right]^*\mathrm{d}x=0,\\ &k=1,2,\ldots,N+M-1,\end{aligned}\tag{22}$$

where $*$ indicates the conjugate complex value. On the basis of formulae (19) and (20) the evaluation of the integrals can be (partly only numerically) executed and

the resulted linear system of equation can be solved. In knowledge of coefficients $\mathbf{C}_n$ the field quantity can be calculated by (19) and (20).

4. Average Errors, Powers

To control the accuracy of the calculation the mean value of the following relative error functions can be created: $\frac{|\mathbf{H}-H_0|}{H_0}$ along the corrugated surface, $\frac{|\mathbf{E}_x|}{|\mathbf{E}_y|}$ along surface $y=0$, and $\frac{|\mathbf{E}_t|}{|\mathbf{E}_n|}$ along the corrugated surface, where $\mathbf{E}_t$ is the tangential component of the electric field intensity along the same surface and $\mathbf{E}_n$ is the normal one. To the calculation of the last quantity let us consider *Fig.2*.

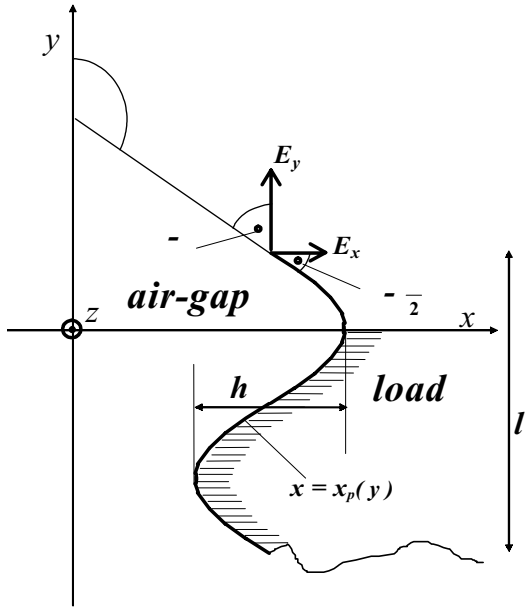

Fig. 2.

$$\mathbf{E}_t = \mathbf{E}_y \cos(\pi - \vartheta) - \mathbf{E}_x \cos\left(\vartheta - \frac{\pi}{2}\right) \equiv -\mathbf{E}_y \cos\vartheta - \mathbf{E}_x \sin\vartheta,$$

$$\mathbf{E}_n = \mathbf{E}_y \cos\left(\vartheta - \frac{\pi}{2}\right) + \mathbf{E}_x \cos(\pi - \vartheta) \equiv \mathbf{E}_y \sin\vartheta - \mathbf{E}_x \cos\vartheta,$$

where

$$\operatorname{tg}\vartheta = x_p'(y) \equiv -\frac{h\pi}{l}\sin\left(\frac{2\pi}{l}y\right), \quad \sin\vartheta = \frac{|\operatorname{tg}\vartheta|}{\sqrt{1+\operatorname{tg}^2\vartheta}}, \quad \cos\vartheta = \frac{\sin\vartheta}{\operatorname{tg}\vartheta}.$$

With the flux of the metal load, induced voltage can be obtained from the line integral of the electric field intensity along the rippled line of metal surface. For the corrugated wavelength it has the form:

$$\begin{aligned}\mathbf{U}_i &= \int_0^l \left[(\mathbf{E}_x)_{x=x_p(y)}\,\mathrm{d}x + \left(\mathbf{E}_y\right)_{x=x_p(y)}\,\mathrm{d}y\right] \\ &= \int_0^l \left[(\mathbf{E}_x)_{x=x_p(y)}\,x_p'(y) + \left(\mathbf{E}_y\right)_{x=x_p(y)}\right]\mathrm{d}y.\end{aligned}$$

However, from formula (9) $x_p'(y) = -\dfrac{h\pi}{l}\sin\left(\dfrac{2\pi}{l}y\right)$, consequently

$$\mathbf{U}_i = \int_0^l \left[\left(\mathbf{E}_y\right)_{x=x_p(y)} - \frac{h\pi}{l}\sin\left(\frac{2\pi}{l}y\right)(\mathbf{E}_x)_{x=x_p(y)}\right]\mathrm{d}y. \tag{23}$$

The voltage $\mathbf{U}$ at the inductor lines (see *Fig. 1*) for a wavelength is:

$$\mathbf{U} = \mathbf{U}_i + j\omega\mu_0 H_0\left(a + \frac{h}{2}\right)l, \tag{24}$$

where the second term is the voltage induced by the air-gap flux. (The integrals of $\mathbf{E}_x$ vanish.)

The complex power per unit surface at the inductor is:

$$\mathbf{S} \equiv P + jQ = \frac{H_0\mathbf{U}}{\ell}. \tag{25}$$

To calculate only the complex specific power intruding through the surface into the conductive half-space which has a plane boundary fitted to the top of the waves (and contains air, see *Fig. 3*)

$$\mathbf{S}_w = P_w + jQ_w, \tag{26}$$

the effective power component remains as it was in (25) ($P_w = P$), but to determine Q_w, it is necessary to subtract the reactive power of the smallest air gap Q_a from Q, so:

$$Q_w = Q - Q_a, \tag{27}$$

where $Q_a = E_0H_0 - E_1H_0 = (E_0 - E_1)H_0$, and according to the induction law:

$$Q_a = H_0^2\omega\mu_0 a = H_0^2\frac{1}{\sigma\delta}\cdot\frac{2a}{\delta}. \tag{28}$$

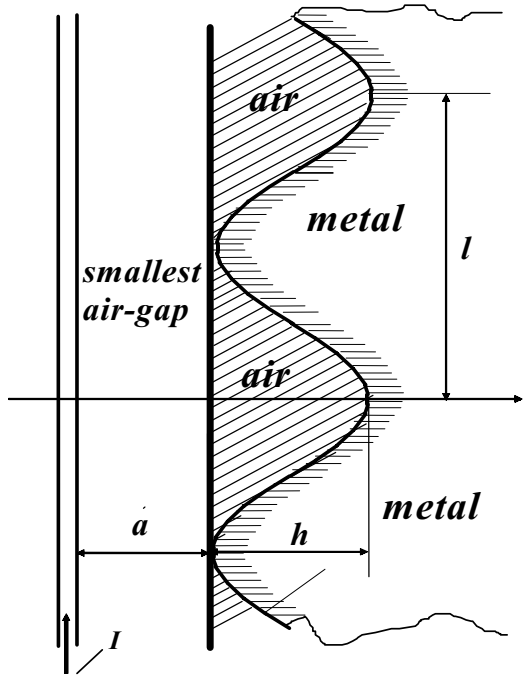

Fig. 3.

The influence of waviness

$$w = \frac{h}{\ell} \tag{29}$$

on the effective and reactive power can be determined by computing the complex power per unit surface ($\boldsymbol{S}_P$) in the case of a plane (zero ripples, $w = 0$) metal surface. According to the known relations:

$$\boldsymbol{S}_p = H_0^2 \frac{1}{\sigma\delta}(1 + j) = P_p + j\,Q_p. \tag{30}$$

Introducing factors

$$\kappa_P = \frac{P_w}{P_p} \tag{31}$$

and

$$\kappa_Q = \frac{Q_w}{Q_p}, \tag{32}$$

they represent the ratio between the effective and reactive power per unit surface of the infinite metal half-space having a corrugated surface closed by a plane and

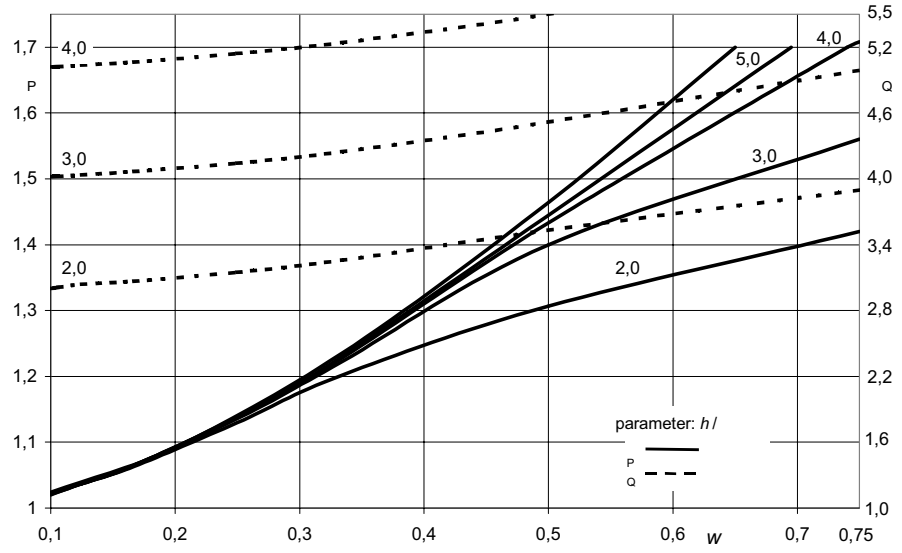

Fig. 4.

the power values of the infinite half-space with a plane surface. Otherwise, these numbers also give the ratio between the components of the complex inner impedance values (AC effective resistances and inner reactance values).

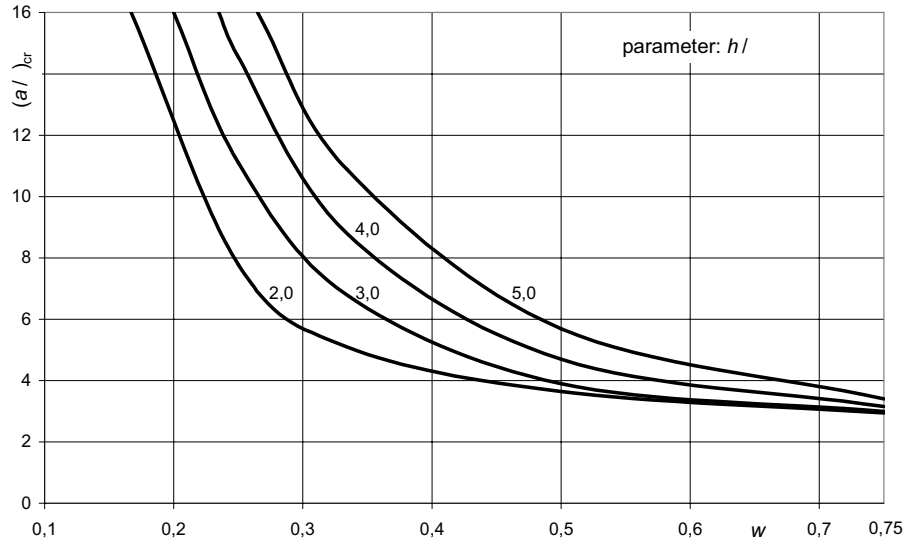

Fig. 5.

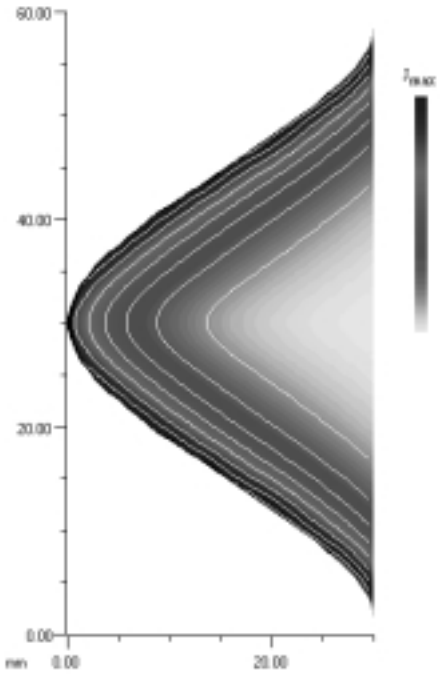

Fig. 6.

Based on the calculation results, it can be seen that κ_P and κ_Q are higher than 1. From the point of induction heating, the first result is advantageous, because it means increasing electrical efficiency of the inductor-load system. The last result seems to be disadvantageous, because it predicts decreasing power factor ($\cos\varphi$) of the inductor-load system. But it must be taken into consideration that the effective power is also greater, furthermore, the generated larger reactive power has a smaller weight in the resultant reactive power because of the reactive power of the additional air gap. To calculate the power factor, it would be necessary to know the complex power generated in the inductor coil, or to know the value of the inner impedance. However, it would be not practical to involve an inductor coil with a difficult geometry into the investigation, because of the simplicity of the computational model. Thus the quantitative comparison of the power factors must be discarded. Therefore our examinations will be done by taking only the air gap into consideration, in the following way. On the basis of formulae (27), (28) and (30) the following resultant reactive power can be obtained for corrugated metal surface in the case of an air gap with a thickness of a:

$$Q = Q_w + 2Q_p \cdot \frac{a}{\delta} \tag{33}$$

and

$$Q' = Q_p \left(1 + 2 \cdot \frac{a}{\delta}\right) \tag{34}$$

for plane surface. Ratio Q/P directly describes the power factor, because if it is smaller, the power factor is greater and vice-versa. Its value for a corrugated surface is

$$\frac{Q}{P_w} = \frac{Q_w}{P_w} + 2\frac{Q_p}{P_w}\frac{a}{\delta},$$

while in the case of a plane metal surface

$$\frac{Q'}{P_p} = \frac{Q_p}{P_p}\left(1 + \frac{2a}{\delta}\right).$$

Using equation $Q_p = P_p$ and formulae (31), (32)

$$\frac{Q}{P_w} = \frac{\kappa_Q}{\kappa_P} + \frac{2}{\kappa_P} \cdot \frac{a}{\delta}$$

and

$$\frac{Q'}{P_p} = 1 + \frac{2a}{\delta}.$$

Both quantities are linear functions of a/δ. In the following it can be seen that

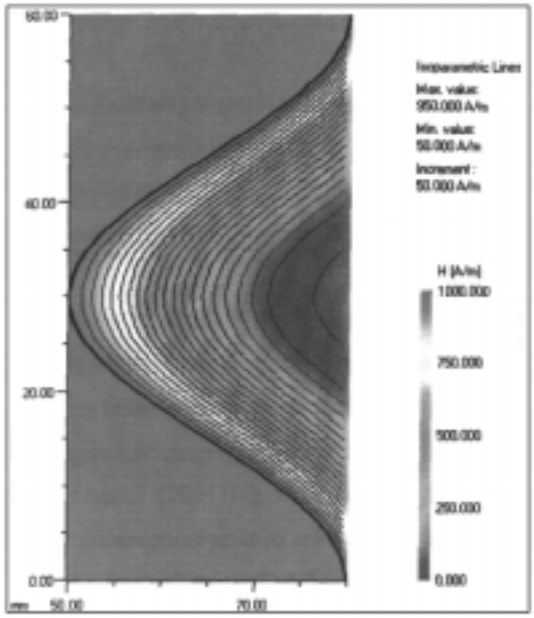

Fig. 7. Isometric lines of magnetic field strength, which are at the same time the field lines of the electric field and the current, when the current of inductor is maximal

$\kappa_Q > \kappa_P$ and $\kappa_P > 1$. Therefore there must be a critical a/δ ratio, where the values of the two quantities are the same:

$$\left(\frac{a}{\delta}\right)_{\text{cr}} = \frac{\kappa_Q - \kappa_P}{2 \cdot (\kappa_P - 1)}. \tag{35}$$

This critical ratio is important because in the case of $\frac{a}{\delta} > \left(\frac{a}{\delta}\right)_{\text{cr}}$ relation $\frac{Q}{P_W} < \frac{Q'}{P_P}$ is valid, so a load with a corrugated surface produces a better power factor.

5. Computational Results, Evaluation

The change of comparative factors (κ_P, κ_Q and $\left(\frac{a}{\delta}\right)_{\text{cr}}$) computed by the presented computational method are plotted in diagrams. The results are plotted as a function of the waviness of the metal surface ($w = h/l$) in domain $0.1 \leq w \leq 0.75$ at different relative wave depths ($h/\delta = 2.0, 3.0, 4.0, 5.0$ and ∞).

In *Fig 4* the change of κ_P and κ_Q can be seen. From the figure it can be learned that in the investigated case both of the factors are increasing with increasing waviness (w) and relative wave depth (h/δ). In the case of parameter $h/\delta = \infty$ the current will flow completely on the corrugated surface and the effective power related to the smooth metal surface can be expressed by the proportion of the length of the sinusoidal curve (s) related to the length of wave (l), so $(\kappa_P)_{h/\delta=\infty} = s/l$.

The primary goal of the application of a load with corrugated surface instead of a plane surface is *to increase the efficiency of the inductor load system by increasing the effective power streaming into the load, namely to obtain as high κ_P value as possible.* Even a large degree of power increment can be achieved. Its largest value would be 86.6% in the case of parameters $w = 0.75$ and $h/\delta = \infty$ ($(\kappa_P)_{h/\delta=\infty} = 1.866$). The increment of the effective power is not too much smaller (77.1%; $\kappa_P = 1.771$), which can be obtained at $w = 0.75$ and $h/\delta = 5.0$. It is very difficult in the practical life to produce much higher values. Taking a glance at *Fig. 3*, practically it is suitable to choose the parameters in domains $0.4 \leq w \leq 1.0$ and $2.0 \leq h/\delta \leq 4.0$.

Fig. 5 represents the change of the critical relative values of the air gap ($\left(\frac{a}{\delta}\right)_{\text{cr}}$). These values are decreasing with increasing w and decreasing h/δ. It can be noticed that *choosing the parameters in domains* $0.4 \leq w \leq 1.0$ *and* $2.0 \leq h/\delta \leq 4.0$ *is useful not only from the point of view of the efficiency of the inductor load system, but from the aspect of the increment of the power factor as well.*

In *Fig. 6* the isometric lines of the current density are plotted in the case of $a/\delta = 10.0$; $w = 0.5$ and $h/\delta = 6.0$. The number of terms are $N = 25$ and $M = 18$, the average error of H, E, $E_{y=0}$ are 1%, 3.29% and 2.08%, respectively. It can be noticed that the isometric lines of the current density practically follow the profile of the waves. Thus, the eddy current must flow through a longer way related

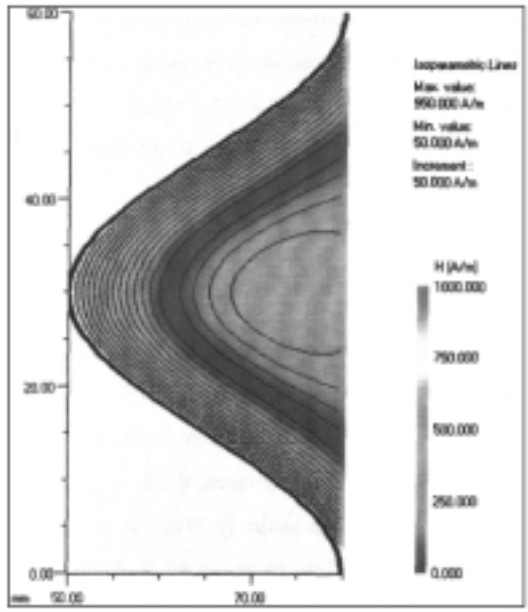

Fig. 8. Isometric lines of magnetic field strength, which are at the same time the field lines of the electric field and the current, when the current of load is maximal

to a plane surface, so the AC effective resistance of the load increases, as well as the effective power generated in the load. *Fig. 7* and *8* represent the magnetic field in two different moments.

Acknowledgements

This publication has been created based on project OTKA 025045.

References

[1] SIMONYI, K., *Foundations of Electrical Engineering*. Oxford: Pergamon Press Ltd. 1963.
[2] KORN, G. A. – KORN, T. M. *Mathematical Handbook for Scientists and Engineers*, Second Enlarged and Revised Edition. McGraw-Hill Book Company, Inc. New York, Toronto, London. (Chapter 20.9.9.)